Waveform Design Methods for Piezo Inkjet Dispensers Based on Measured Meniscus Motion

Kye-Si Kwon

Abstract—**Waveform design methods for piezo inkjet dispensers based on measured meniscus motion are presented. The meniscus motion is measured from charge-coupled-device camera images wherein strobe lights from light-emitting diodes are synchronized with the jetting signal. Waveforms for the piezo dispenser are designed such that the number of experiments can be significantly reduced compared to conventional methods. Furthermore, the designed waveform can also be evaluated by the measured meniscus motion since the motion is directly related to jetting behavior. [2009-0032]**

Index Terms—**Measurement.**

I. Introduction

INKJET technology has recently emerged as one of the most powerful tools for patterning electronic applications such as large-area displays, radio-frequency identification, and printed-circuit-board patterning [1]–[3]. As inkjet applications broaden, various types of jetting materials are required to be precisely dispensed from the inkjet head. Jetting fluids need to have jettable material properties, as discussed in [4] and [5]. In addition, jetting performance needs to be well controlled for inkjet technology to be viable in various applications. To control jetting performance parameters such as droplet speed and droplet volume, the input waveform voltage driving the printhead must be properly designed [6]–[9]. In practice, a simple trapezoidal waveform has been widely used for this purpose. To find the optimal dwell time for the waveform, the relationship between droplet jetting speed and dwell time has been sought [6]–[8]. However, this conventional approach for designing the waveform requires a number of experiments to scan the dwell time for its relationship to droplet jetting speed. Furthermore, if there is no jetting from inkjet dispensers, it is difficult to understand the possible causes of nonjetting. In such cases, a trial-and-error approach has been the only option to determine the jetting conditions. In this paper, a new waveform design method is proposed such that time-consuming efforts to find optimal waveforms can be reduced.

Since the experimental study by Bogy and Talke [7], jetting phenomena have been known to be related to a pressure wave of the ink inside the inkjet head. In the paper by Bogy and Talke, meniscus-protrusion behavior was discussed in relation to pressure waves. However, an in-depth study of meniscus motion behavior might be difficult because the meniscus measurement in the paper by Bogy and Talke relied on postprocessing a prohibitively large number of charge-coupled-device (CCD) camera images.

Recently, the meniscus motion in an inkjet nozzle was measured using particle tracking velocimetry (PTV) or particle image velocimetry (PIV) techniques [10], [11]. Using visualization, the jetting behavior can be understood. However, additional particles, which might change jetting performance, must be included for PIV measurement. Also, special equipment is required for particle velocity measurement. In summary, measurement methods based on PIV or PTV may not be quick and simple enough for meniscus motion measurement and waveform design in industrial printing devices.

In this paper, a new method for measuring meniscus motion is proposed. The proposed technique uses a CCD camera system wherein light-emitting-diode lights are synchronized with the jetting signal. Therefore, the proposed method does not require special hardware, unlike previous methods using PIV techniques. Most printing systems already have a CCD camera system with a strobe LED for measuring droplet speed [1], [7]–[9]. Therefore, only software algorithms need to be implemented in existing CCD camera systems for *in situ* measurement of meniscus motion. The proposed software algorithm has two parts: 1) image processing to identify the meniscus location from the CCD camera image and 2) controlling LED lights that enable CCD camera image acquisitions of the meniscus motion over the duration of interest after the jetting signal. The measurement of meniscus motion has the advantage that jetting behavior can be predicted without actual jetting.

As an application of the measured meniscus motion, a waveform design method is presented. It should be noted that the motion is likely to be complex because it is the combined result of pressure waves generated from both the rising and falling sections of the waveform. For straightforward analysis of meniscus motion behavior in relation to a waveform, the use of a trial waveform with a long dwell time is proposed. By using the test waveform, meniscus motion from either the rising or the falling region of the waveform can be analyzed separately. From the period of the measured motion, the optimal value for the dwell time of the waveform can be determined. Dwell time is known to be one of the critical parameters in designing a waveform [6]–[8]. The proposed waveform design scheme will be extended to a waveform for high-frequency jetting; this requires two optimal values for dwell time since there are two dwell components in the waveform. Finally, the jetting behavior of a negative waveform will be discussed.

Manuscript received February 2, 2009; revised April 30, 2009. First published July 31, 2009; current version published September 30, 2009. Subject Editor Y. Zohar.

The author is with the Department of Mechanical Engineering, Soonchunhyang University, Asan 336-745, Korea (e-mail: kskwon@sch.ac.kr).

Color versions of one or more of the figures in this paper are available online at http://ieeexplore.ieee.org.

Digital Object Identifier 10.1109/JMEMS.2009.2026465

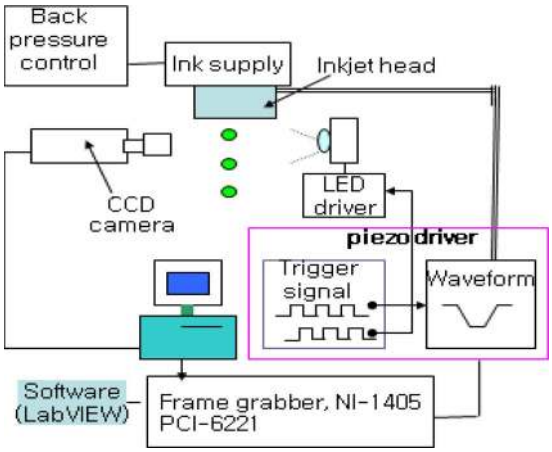

Fig. 1. Experimental setup.

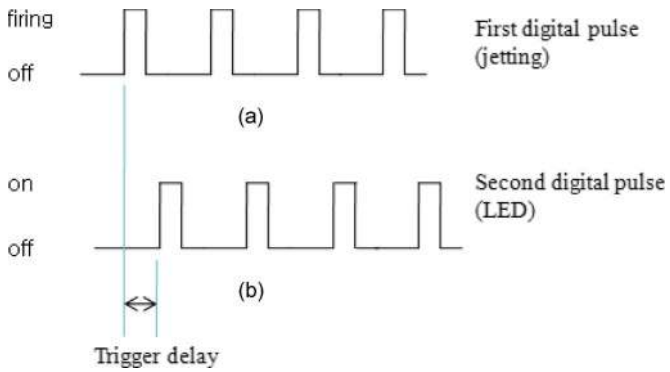

Fig. 2. Digital pulse trains.

II. Measurement of Meniscus Motion

Fig. 1 shows a schematic of a typical drop watcher system for acquiring strobe CCD camera images in order to measure droplet jetting speed and droplet volume [1], [7]–[9]. Here, LED lights, which are synchronized with the jetting signal, are used to acquire frozen droplet images [12]. To control the LED lights, two digital pulses are generated and controlled in this paper. The first digital pulse train, shown in Fig. 2(a), is used as a trigger signal for jetting. The second pulse train, shown in Fig. 2(b), is used for controlling the LED light. The second pulse was triggered from the first pulse, and the trigger delay with respect to the first digital pulse was controlled. By adjusting the delay time of the second digital pulse with respect to the first pulse, the frozen image at the delay time can be obtained. To measure droplet speed, two preset delay times in the second digital pulse were used [12]. However, a number of predetermined sets of delay times for controlling the LED lights are required for measuring meniscus motion. At each delay time, the meniscus location will be determined via image-processing techniques. In this paper, so-called edge detection techniques were used to identify the meniscus location. Edge detection techniques have been used in many vision applications where information about the location of object boundaries is required [12]. To apply the edge detection technique to meniscus motion measurement, a straight-line region of interest (ROI) generated near the nozzle in the jetting direction was used for CCD camera image analysis. Then, the meniscus location was identified from the discontinuity in the pixel intensities along the ROI in the acquired image. The ROI line consists of image pixels having values that vary from 0 to 255 according to the brightness of the image. Meniscus locations can be detected by setting a suitable threshold value where the image pixel values in the ROI will cross the threshold value. This image processing should be repeated in order to obtain each meniscus location at predetermined sets of delay times for the LED lights. Note that this method measures only the protruding meniscus. Therefore, information can be lost if the meniscus is hidden inside the nozzle.

Fig. 3 shows the software that we developed to automatically measure meniscus motion. For a better understanding of the software, a video clip can be found from the Web site in [13]. Unlike the jetted-droplet speed measurement, a low magnitude of input voltage should be used to prevent the printhead from jetting any ink droplets.

A single nozzle head (MJ-AT-01-50) from MicroFab Technologies, Inc., which has an orifice diameter of 50 μm, was used as the jetting device for the experiment. For the jetting material, we used a nanosilver ink with nanoparticles dissolved in deionized water.

The accuracy of the measured meniscus motion depends mainly on the image resolution. For our imaging system, a Sony XC ES 50 system was used to acquire images. Here, a lens (MORITEX-ML-Z07545) and a lens adaptor (MORITEX-ML-Z20) were used to obtain the required magnified image. As a result, one pixel in the CCD camera image corresponds to about 1.3 μm. The resolution can be increased by adjusting the magnification of the lens or by replacing the CCD camera with a high-resolution camera with more pixels in the camera sensor. We note that the measured results can also be affected by various conditions such as lighting, lens focus, and the threshold value for detecting meniscus location. Nonetheless, the accuracy of the measured meniscus motion may not be critical in this paper because the proposed algorithm for waveform design uses the period of the measured meniscus motion.

III. Waveform Design Based on Measured Meniscus Motion

A. Conventional Method for Designing Waveform

In this section, we discuss a conventional waveform design method for determining the waveform parameters of the trapezoidal waveform shown in Fig. 4. The results from the conventional method will then be compared with the results from the proposed waveform design method.

When the rising (or falling) section of the waveform shown in Fig. 4 is applied to a piezo inkjet dispenser, negative (or positive) pressure waves are generated and then propagate inside the dispenser tube [7]. On the other hand, the dwell region of the waveform is not related to the generation of pressure waves but rather to the amplification or cancellation of pressure waves generated from the rising and falling sections of the waveform. Ink droplet jetting becomes easier if the positive pressure wave is amplified by means of adjusting the dwell time.

To control the jetting performance of inkjet dispensers, the parameters of the waveform, shown in Fig. 4, must be properly

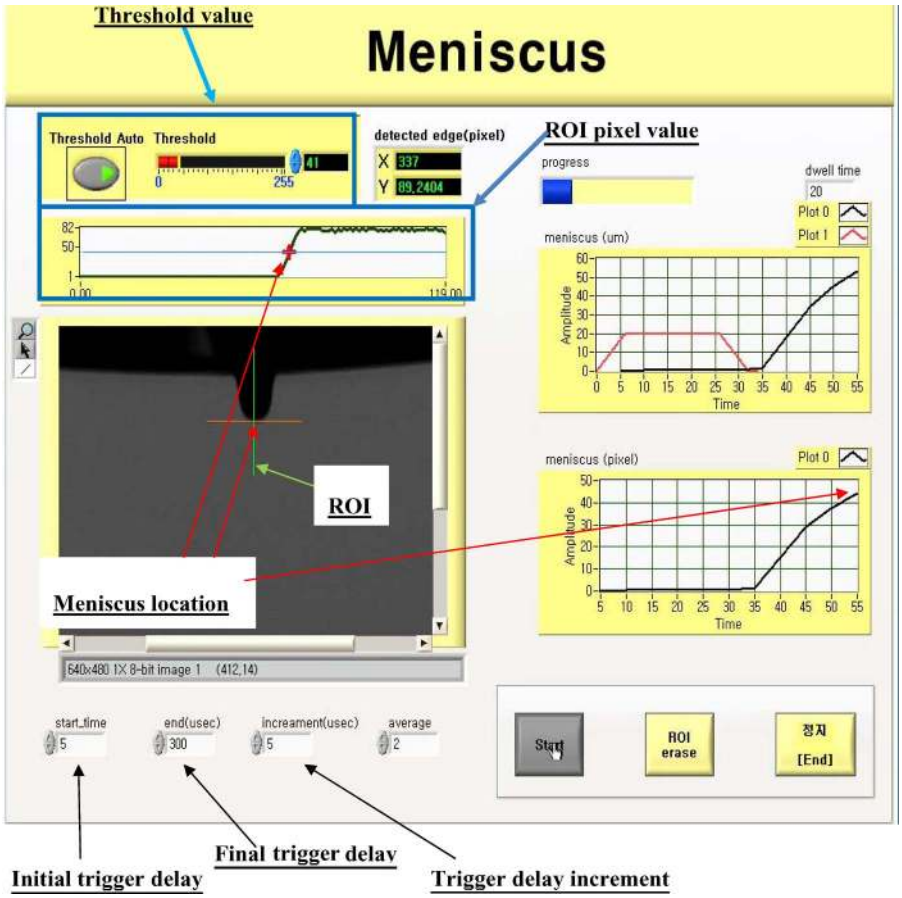

Fig. 3. Developed software for measuring meniscus motion [13].

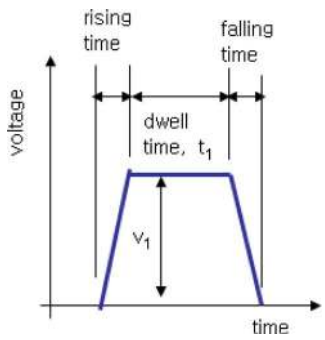

Fig. 4. Trapezoidal waveform.

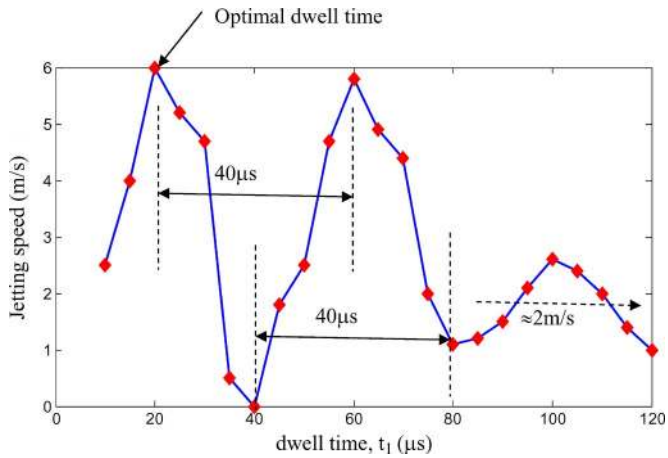

Fig. 5. Droplet-jetting-speed and dwell-time relationship ($v_1 = 30$ V).

determined. Normally, a fixed value for both the rising and falling times is used [7]. Thus, the waveform design issue is focused on determining the optimal value for dwell time. An optimum value for dwell time of L/C, where L is the dispenser tube length and C is the speed of sound of the ink, was recommended in [7] and [8] for the amplification of the positive pressure wave of the ink inside an inkjet dispenser. For practical application, the optimal value of dwell time has been determined by experimental means in [6]. For this purpose, the droplet-jetting-speed and dwell-time relationship was sought by measuring the droplet jetting speed using a strobe LED [6], [8]. Fig. 5 shows the experimental results for the speed and dwell-time relationship when the magnitude of the waveform and rising/falling time were fixed at 30 V and 6 μs, respectively.

From Fig. 5, the optimal dwell time t_1 can be designed to be 20 μs when the maximum speed is obtained. Then, as a final step, the magnitude of voltage v_1 can be determined by measuring the jetting speed. Here, higher voltage would result in higher droplet speed and vice versa.

The measured jetting-speed and dwell-time relationship contains considerable information on jetting behavior. From the results shown in Fig. 5, the jetting speed has peaks with a period of 40 μs with respect to the dwell time. The period is related to the speed of sound of the ink. The effect of the first rising

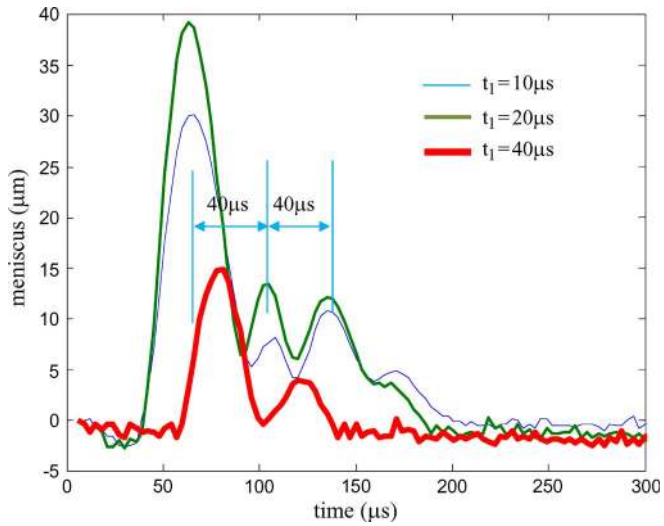

Fig. 6. Meniscus motion with different dwell times ($v_1 = 15$ V).

section of the waveform will decay due to the damping effect of the pressure wave if a waveform with a long dwell time is used. As a result, the peaks of the droplet speed shown in Fig. 5 became smaller as the dwell time increased. Therefore, the damping effect of the pressure wave can also be understood. Note that the jetting speed converged to 2 m/s with the increase in dwell time because the effect of the falling section of the waveform dominated when the dwell time was long.

This conventional method of waveform design needs many experiments to obtain the speed versus dwell-time relationship. The measurement is based on the speed of jetted droplets. If there is no jetting, a trial-and-error approach must be used to find the appropriate jetting conditions.

B. Basic Waveform Design Based on Meniscus Motion

In this section, a new waveform design method based on measured meniscus motion is discussed.

For waveform design based on meniscus motion, a proper trial waveform should be used. Otherwise, it may be difficult to extract useful information from the measured meniscus motion. Fig. 6 shows the measured meniscus motions from arbitrary trial waveforms. As seen in the figure, meniscus behaviors differ by waveforms because traveling pressure waves from the rising and falling sections of the waveforms interact with each other. As a result, meniscus behavior in response to the waveform was difficult to be understood.

For a proper trial waveform, we recommend the use of a waveform with a very long dwell time. The trial waveform has the same form as the basic waveform shown in Fig. 4, except that it has a longer dwell time. During the long dwell time, the piezo actuator in the inkjet dispenser is not actuated; thus, the meniscus behavior from the first rising section of the waveform can be observed without interference with the final falling section. In addition, during the long dwell time, pressure waves from the rising section of the waveform are likely to decay due to the damping of the pressure waves. As a result, meniscus motion due to the latter falling section can also be understood. Fig. 7(a) shows the meniscus behavior from the

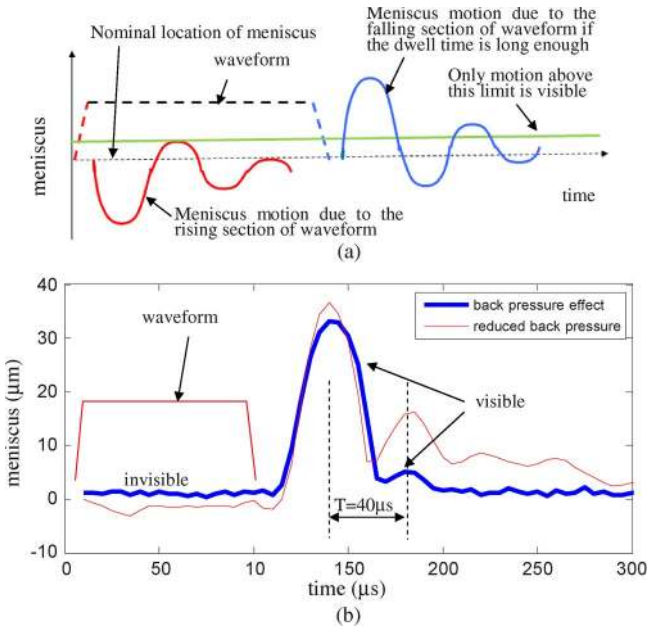

Fig. 7. Meniscus motion from the positive trial waveform with long dwell time ($v_1 = 17$ V and $t_1 = 100$ μs). (a) Meniscus behavior from the positive trial waveform. (b) Measured meniscus motion.

trial waveform. Here, the dwell time for the trial waveform should be long enough so that at least two peaks of the meniscus can be observed, and the damping effect can reduce meniscus oscillation significantly before subsequent piezo actuation from the final falling section of the waveform. From two peaks of meniscus motion, period T of the meniscus can be measured. Here, the meniscus period of the ink is inversely proportional to the speed of sound of the ink.

Fig. 7(b) shows the measured meniscus motion from a trial waveform with a dwell time of 100 μs. The meniscus motion related to the rising section of the waveform, as seen in Fig. 7(b), was difficult to measure since a generated negative pressure wave due to the first rising section pulled the meniscus location into the nozzle. Later, when the falling section of the waveform was applied, the meniscus motion was visible for a while since a positive pressure wave can push the meniscus out from the nozzle. In our experiment, the protruded-meniscus location tended to be hidden inside the nozzle, as seen in Fig. 7(b), due to the so-called meniscus vacuum (or back pressure). The meniscus vacuum, which is a small negative pressure applied at the ink reservoir, is needed because it can prevent weeping of the ink from the nozzle. Nonetheless, it can be observed from Fig. 7(b) that the period of meniscus motion from the trial waveform T was about 40 μs. However, the period of meniscus motion may be difficult to measure in some cases. Then, the negative back pressure can be intentionally reduced for measuring meniscus motion, as shown in Figs. 7(b) and 8(b).

Negative voltage can be used for a trial waveform, as shown in Fig. 8. Since the first falling section of the waveform accounts for the positive pressure wave, protruded-meniscus motion can be measured first, as shown in Fig. 8(b). Here, the period of the meniscus motion T can be measured as 40 μs, which is in good agreement with the result shown in Fig. 7(b). The

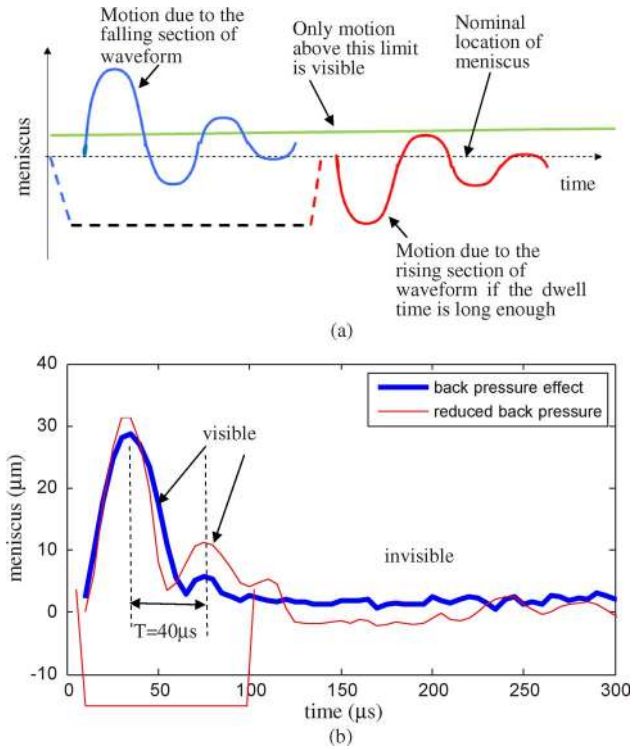

Fig. 8. Meniscus motion from the negative trial waveform with long dwell time ($v_1 = -17$ V and $t_1 = 100$ μs). (a) Meniscus behavior from the negative trial waveform. (b) Measured meniscus motion.

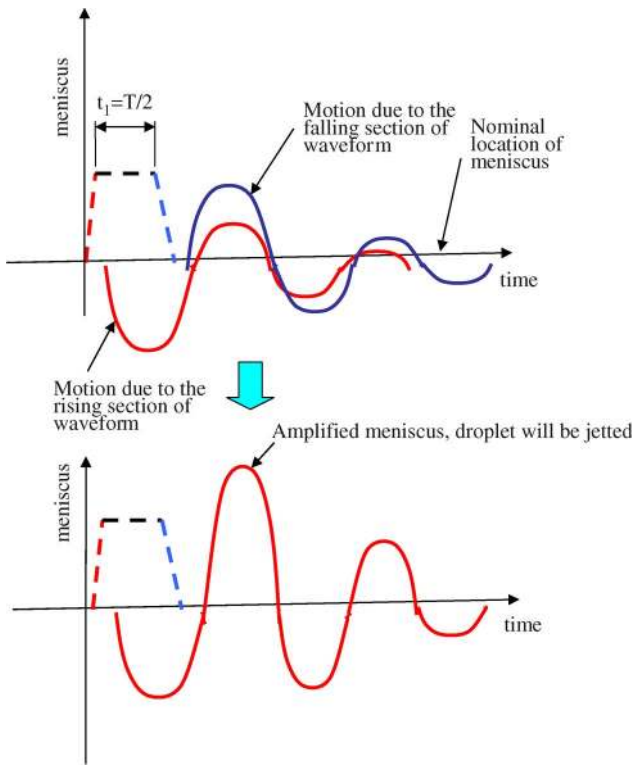

Fig. 9. Meniscus behavior from the optimal waveform.

use of a negative trial waveform can have advantages since the first measured meniscus motion is likely to be the result of the pressure wave generated from the first falling section of the waveform only. In the previous positive trial voltage, shown in Fig. 7, the protruded-meniscus motion due to the final falling section of the waveform may be subject to the first rising section, even though the meniscus oscillation from the first rising section is damped.

Once the period of meniscus motion from either the rising or falling section of the waveform is measured, the optimal dwell time can be easily determined. Assuming that the pressure waves (or meniscus oscillation) from the rising and falling times have the same period with a phase difference of 180°, the positive meniscus can be maximized by setting the dwell time to a one-half period of the measured meniscus motion, as shown in Fig. 9. Therefore, the optimal value for dwell time was determined to be 20 μs ($t_1 = T/2$), which is in good agreement with the optimal dwell time from the speed and dwell-time relationship shown in Fig. 5. The jetting behavior can then be predicted without actual jetting by measuring the meniscus motion. For example, Fig. 6 shows the meniscus motion from the waveform with optimal dwell time $t_1 = 20$ μs. By observing the meniscus motion, we see that jetting will likely occur at 60 μs after the jetting signal is applied. Later, the second meniscus peak at 100 μs is likely to become a satellite drop if the magnitude of the waveform becomes large.

As a final step in waveform design, the magnitude of the waveform was determined such that the target droplet jetting speed can be satisfied. The magnitude of meniscus motion is related to jettability of the jetting materials. If the magnitude of the meniscus motion of the jetting material is small, a higher waveform voltage may be needed for jetting.

Note that a dwell time that is equal to the period of meniscus motion can cancel the pressure waves since the phase of the pressure waves from the rising and falling sections of a waveform is 180°. As shown in Fig. 5, the droplet speed was reduced significantly when the dwell time approached 40, 80, 120 μs, etc., which is repeated due to the periodicity in meniscus behavior.

C. Waveform Design for High-Speed Jetting

For reliable jetting, a subsequent droplet should not be ejected until the meniscus vibration from the previous drop has sufficiently decayed. This damping takes time and limits the maximum jetting frequency. High-frequency jetting is required to increase the speed of printing. To obtain higher frequency jetting, a proper waveform for the dispenser needs to be designed such that residual meniscus oscillation can be effectively suppressed after droplet jetting [14].

Compared to a basic waveform, more parameters, including two optimal dwell times, are required to determine a waveform, such as that shown in Fig. 10 for high-frequency jetting [6], [9]. The first dwell time t_2 is related to jetting, as discussed in the previous section. In addition, it was found that the optimal value for maximizing jetting pressure is one-half of the measured meniscus period from the trial waveform; i.e., $t_2 = T/2$. The second dwell time t_3 is related to the suppression of residual meniscus oscillation after jetting.

The effect of the first dwell time t_2 can be understood from the conventional approach using droplet jetting speed, as shown

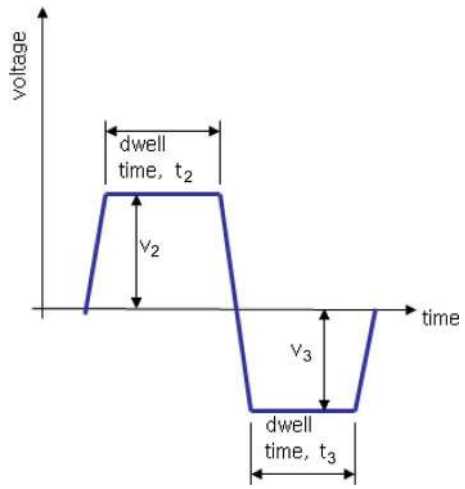

Fig. 10. Waveform for high-speed jetting.

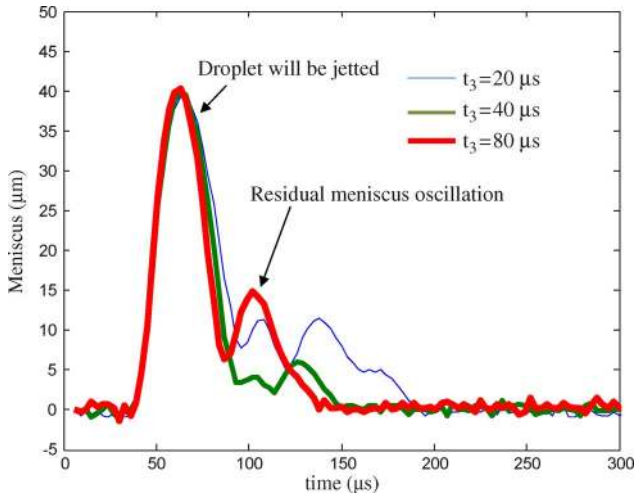

Fig. 11. Meniscus oscillation from the waveform for high-speed jetting ($t_2 = 20\ \mu$s, $v_2 = 8$ V, and $v_3 = 8$ V).

in Fig. 5. However, the effect of the second dwell time t_3 may be difficult to understand from the droplet speed measurement.

To understand the residual pressure-wave behavior, a self-sensing capability was used in previous works [14], [15]. By measuring the pressure-wave behavior, the waveform can be generated by maximizing jetting pressure and minimizing residual pressure waves [14], [15]. However, an additional circuit for measuring the pressure-wave signal needs to be implemented, which may be difficult in some commercial piezo inkjet printheads. As an alternative, the use of measured meniscus motion is presented not only for determining the optimal value of dwell times but also for evaluating the designed waveform. The use of measured meniscus motion can be straightforward since it is directly related to jetting behavior. Fig. 11 shows the effect of the second dwell time t_3 on residual meniscus motion. We recommend that the optimal value for the second dwell time be the period of the measured meniscus motion from the trial waveform, as shown in Fig. 12, which was 40 μs ($t_3 = \mathrm{T}$) in this paper. The suppression effect shown in Fig. 11 ($t_3 = 40\ \mu$s) can be understood by comparing the measured meniscus motions from waveforms with different

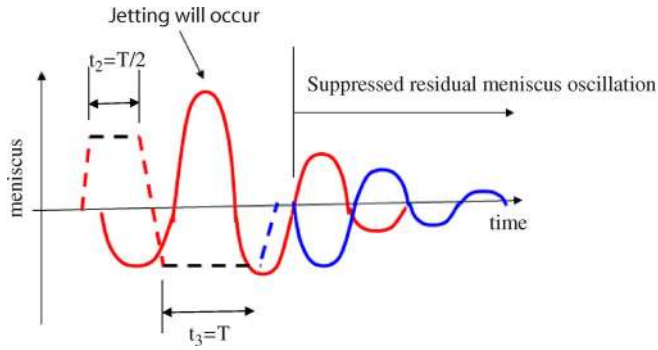

Fig. 12. Meniscus behavior from the optimal waveform for high-frequency jetting.

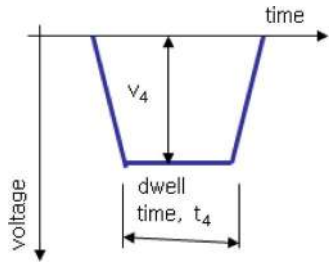

Fig. 13. Negative waveform.

second dwell times ($t_3 = 20$ and $80\ \mu$s). Note that the second dwell section of the waveform is unlikely to affect jetting, as seen in Fig. 11.

As a final step in designing the waveform, appropriate voltages in the waveforms v_2 and v_3 will be determined based on the measured jetting speed and residual meniscus oscillation.

D. Negative of Basic Waveform

To the author's knowledge, few research papers have discussed a negative waveform that has the opposite sign of the basic waveform, as shown in Fig. 13. The use of a negative waveform may be straightforward because the first falling section of the waveform alone can result in jetting. Later, the rising section of the negative waveform is needed to restore the input voltage to zero for the next firing. Consequently, the dwell time of the waveform seems to be unimportant in terms of jetting. Fig. 14 shows the relationship between dwell time and speed of the negative waveform. The droplet speed remains relatively constant, which is independent of the dwell time. However, the droplet speed decreased from 6 to around 2 m/s compared to that of the basic waveform in Fig. 5. Therefore, we suggest that the use of negative waveform should be limited to jetting fluids with high jettability.

Even though jetting speed is less sensitive to dwell time, the waveform needs to be carefully designed. In designing a negative waveform, a dwell time of 40 μs ($t_4 = T$) is recommended for canceling residual pressure waves, as shown in Fig. 15. The measured residual meniscus behavior in Fig. 16 might look trivial since the only protruding part was measured. However, the negative pressure from the rising section of the waveform often results in poor jetting conditions since the negative pressure from the final rising section may pull

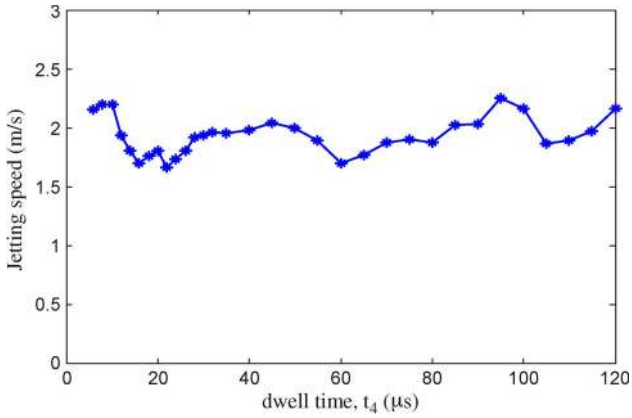

Fig. 14. Droplet-speed and dwell-time relationship using the negative waveform ($v_4 = 30$ V).

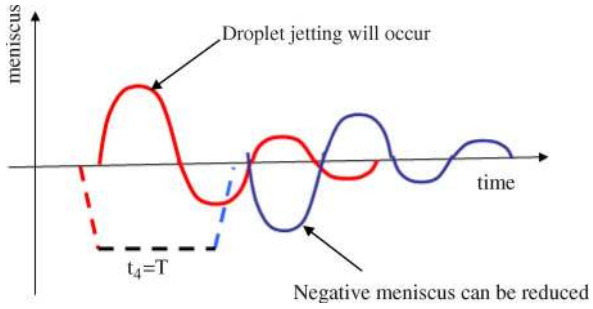

Fig. 15. Meniscus behavior from the optimal negative waveform.

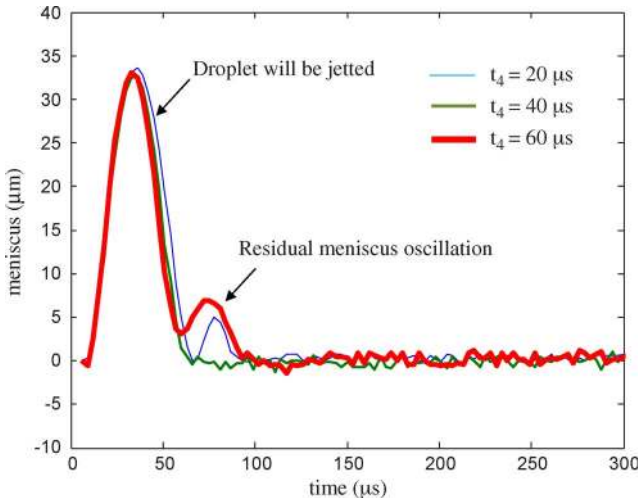

Fig. 16. Measured meniscus motion from the negative waveform ($v_4 = 19$ V).

the meniscus into the nozzle excessively in some cases; e.g., $t_4 = T/2, 3T/2$, etc.

IV. Discussion and Conclusion

New measurement techniques have been presented to measure inkjet meniscus motion using a CCD camera system with strobe LEDs. Jetting behavior can be predicted from the meniscus motion. To analyze the waveform effect on meniscus motion, the use of a trial waveform with a long dwell time was proposed. Based on the measured meniscus period, the optimal value for dwell time in the waveforms can easily be determined. The results can be summarized as follows.

1) In the basic waveform, the optimal value of dwell time is one-half of the measured meniscus period ($t_1 = T/2$).
2) In a waveform for high-frequency jetting, the optimal value of the first dwell time is one-half of the meniscus period for jetting ($t_2 = T/2$), whereas the optimal value for the second dwell time is the meniscus period in order to suppress residual meniscus oscillation ($t_3 = T$).
3) For a negative waveform, the optimal value for dwell time is the meniscus period in order to reduce undesirable residual meniscus oscillation ($t_4 = T$).

By using the proposed method for measuring meniscus motion and the proposed waveform design algorithm, experimental efforts needed to determine optimal dwell time can be reduced. In addition, the designed waveform can be evaluated using meniscus motion without the need for actual jetting since the jetting behavior can be predicted from the measured motion.

The proposed method was focused on designing an efficient waveform, which can result in maximum meniscus motion for jetting and minimum residual meniscus motion after jetting. On the other hand, once ink droplets are jetted from the nozzle, other issues arise such as satellite droplets, droplet volume, and jetting directionality due to nozzle surface wetting. The optimization of such droplet jetting conditions is beyond the scope of this paper and requires further research.

Acknowledgment

The author would like to thank J.-H. Myung for the assistance with experiments.

References

[1] D. Albertalli, "Gen 7 FPD inkjet equipment—Development status," *SID Symp. Dig. Tech. Pap.*, vol. 36, no. 1, pp. 1200–1203, May 2005.
[2] D. Redinger, S. Molesa, S. Yin, R. Farschi, and V. Subramanian, "An ink-jet-deposited passive component process for RFID," *IEEE Trans. Electron Devices*, vol. 51, no. 12, pp. 1978–1983, Dec. 2004.
[3] S. B. Fuller, E. J. Wilhelm, and J. M. Jacobson, "Ink-jet printed nanoparticle microelectromechanical systems," *J. Microelectromech. Syst.*, vol. 11, no. 1, pp. 54–60, Feb. 2002.
[4] J. E. Fromm, "Numerical calculation of the fluid dynamics of drop-on-demand jets," *IBM J. Res. Develop.*, vol. 28, no. 3, pp. 322–333, May 1984.
[5] N. Reis, C. Ainsley, and B. Derby, "Ink-jet delivery of particle suspensions by piezoelectric droplet ejectors," *J. Appl. Phys.*, vol. 97, no. 9, p. 094 903, Apr. 2005.
[6] "Drive waveform effects on ink-jet device performance," MicroFab Technologies, Inc., Plano, TX, MicroFab Technote 99-03, 1999.
[7] D. B. Bogy and F. E. Talke, "Experimental and theoretical study of wave propagation phenomena in drop-on-demand ink jet devices," *IBM J. Res. Develop.*, vol. 28, no. 3, pp. 314–321, May 1984.
[8] J. B. Szczech, C. M. Megaridis, and D. R. Gamota, "Fine-line conductor manufacturing using drop-on demand PZT printing technology," *IEEE Trans. Electron. Packag. Manuf.*, vol. 25, no. 1, pp. 26–33, Jan. 2002.
[9] J. Chung, S. Ko, C. P. Grigoropoulos, N. R. Bieri, C. Dockendorf, and D. Poulikakos, "Damage-free low temperature pulsed laser printing of gold nanoinks on polymers," *Trans. ASME, J. Heat Transf.*, vol. 127, no. 7, pp. 724–732, Jul. 2005.
[10] B. Beulen, J. D. Jong, H. Reinten, M. V. D. Berg, H. Wijshoff, and R. V. Dongen, "Flows on the nozzle plate of an inkjet printhead," *Exp. Fluids*, vol. 42, no. 2, pp. 217–224, Feb. 2007.

[11] C. D. Meinhart and H. Zhang, "The flow structure inside a microfabricated inkjet printhead," *J. Microelectromech. Syst.*, vol. 9, no. 1, pp. 67–75, Mar. 2000.
[12] K. S. Kwon, "Speed measurement of ink droplet by using edge detection techniques," *Measurement*, vol. 42, no. 1, pp. 44–50, Jan. 2009.
[13] K. S. Kwon, Meniscus Motion Measurement2009. [Online]. Available: http://www.youtube.com/watch?v=U48a7bRtJ9I
[14] K. S. Kwon, "A waveform design method for high-speed inkjet printing based on self-sensing measurement," *Sens. Actuators A, Phys.*, vol. 140, no. 1, pp. 75–83, Oct. 2007.
[15] M. B. G. Wassink, M. J. M Bosch, O. H. Bosgra, and S. Koekebakker, "Enabling higher jet frequencies for an inkjet printhead using iterative learning control," in *Proc. IEEE Conf. Control Appl.*, Toronto, ON, Canada, Aug. 28–31, 2005, pp. 791–796.

Kye-Si Kwon received the B.S. degree in mechanical engineering from Yonsei University, Seoul, Korea, in 1992, and the M.S. and Ph.D. degrees in mechanical engineering from Korea Advanced Institute of Science and Technology, Daejeon, Korea, in 1994 and 1999, respectively.

He has been an Assistant Professor in the Department of Mechanical Engineering, Soonchunhyang University, Asan, Korea, since 2006. Before joining Soonchunhyang University, he was a member of the Research Staff at Samsung Advanced Institute of Technology, Yongin, Korea. His current work includes ink jetting control.